Pergamon

Bioorganic & Medicinal Chemistry Letters, Vol. 4, No. 18, pp. 2211-2216, 1994

0960-894X/94 $7.00+0.00

0960-894X(94)00314-9

A COMPARATIVE MOLECULAR FIELD ANALYSIS DERIVED MODEL OF THE BINDING OF TAXOL® ANALOGUES TO MICROTUBULES[1]

Karl-Heinz A. Czaplinski and Gary L. Grunewald*
Department of Medicinal Chemistry, University of Kansas, Lawrence, KS 66045

Abstract: We investigated a series of Taxol® (**1**, paclitaxel) analogues using a 3-D QSAR approach (CoMFA). Published and unpublished data for more than 50 compounds have been included in the analysis and the model has been used to predict the activity of other analogues. The model accurately describes known SARs and also has good predictive power.

As a guide to the design of new and more potent analogues of the anticancer drug **1**, a 3-D QSAR model (CoMFA[2]) was developed using a training set of 49 analogues of **1** and the biological activities for binding to microtubules. Further, the biological activities of an additional 47 analogues were predicted from the model. See **Figure 1** and **Table 1**. Structures and activity data[3] were taken from a review[4] and from unpublished results[5] by Georg and coworkers.

Comparative Molecular Field Analysis (CoMFA).

Analogues with a variety of different substituents at C-7, C-10, and C-13 were included in this investigation. Structures used in the CoMFA analysis were constructed with the SYBYL[6] software package based on the energy minimized structure of Taxotere® (**39**, docetaxel) taken from the Cambridge Crystallographic Database.[7] Each starting structure was then energy minimized using the MAXIMIN2 force field with Gasteiger-Hückel charges (termination: gradient 0.05 kcal/mol). Finally the atomic charges of all compounds were calculated with the AM1 method.[8] The minimum energy structures of all compounds were aligned by least-squares fitting of carbon atoms 1-15, 20, and oxygen atom 5 of the diterpene skeleton of each structure to the same 17 atoms of **39** using the FIT option of SYBYL.

The aligned structures of all compounds were then submitted to the CoMFA approach. First all superimposed molecules were placed in a three dimensional box containing a grid with a spacing of 2 Å. This region extended the shape of each molecule by at least 4 Å. Then the steric (van der Waals) and electrostatic (coulombic) interaction energies were sampled using an sp^3 hybridized carbon (charged +1) as a probe atom at each intersection point of the three dimensional lattice.

To evaluate the optimal number of components and the predictive power of the resulting model an initial partial least squares (PLS) run with cross validation was calculated with ten components using both CoMFA fields. Any grid point for which the standard deviation of the energies was less than 2.0 kcal/mole was discarded to decrease the background noise and the number of CoMFA columns. Once the optimal number of components was determined by examination of the standard error, a second PLS run with no validation was calculated to yield the final model. The statistical results are shown in **Table 2**.

Results.

The results of the non-validated PLS runs were examined graphically (see **Figures 2** and **3** for model **b6**; the structure of docetaxel is used with no protons on the skeleton for clarity) and by prediction of the activity of compounds not included in the training set [See **Table 3**; the table also includes predicted results for three other models (**wb4**, **e4**, **s4**) not discussed in this paper.[9]]. The resulting maps of the

electrostatic and the steric field of model **b6**[9] demonstrate, that in this data set, substituting the hydroxy functions at C-7 or C-10 has only a minor influence on the activity of the compounds in the microtubule assay. Most interactions take place around the phenyl isoserine side chain. Here, one important site is the 2'-hydroxy moiety, where, after esterification, a negative steric interaction was found by the CoMFA approach to give less active compounds like the 2'-acetylated analogues (**67**, **68**) or the analogues where the 2'-hydroxy and 3'-amide functions have been interchanged (**32**, **34**, **35**, **36**). Literature data[10] showed that R_3'=Ph is better than smaller (*e.g.*, H); the CoMFA results indicate that further substitution on the Ph at R_3' is detrimental (for steric reasons) with the exception of 4-MeO-Ph and 4-HO-Ph (**24**, **25**). Substitution at position R_3" is optimal for *t*-BOC-NH (**39**). For the subset of R_3"=4-X-BzNH, the potency order increases as Hansch π_x and σ_p decrease [**54**(X=CF_3), **47**(X=Cl), **51**(X=Me), **1**(X=H), **55**(X=MeO)]. [See also the predicted values for **43** (X=NO_2), **45** (X=F) and **64** (X=N_3) in **Table 3**].

Discussion.

The information extractable from the steric and electrostatic maps of the CoMFA model **b6**[9] is in good agreement with the results of reported structure activity relationships (SARs) (for a review of SARs see reference 4 and references cited therein) and may be useful as a graphical summary of the SARs reported to date. A disadvantage of the used data set is the small range in the variation of the structural properties of the paclitaxel (**1**) analogues (all include the oxetane ring and 4-acetyl and 2-benzoyl moieties), for which microtubule binding data were available.

The region of unfavorable steric interaction around the 2'-hydroxy group might actually represent a hydrogen bond interaction as reported by Kant and coworkers[11] or might at least incorporate that information to some extent. The predicted activity of 2'-deoxypaclitaxel (**90**) was about ten times too small compared to the actual value (actual ratio: 21.2).[12] A hydrogen bond interaction could also explain the higher activity of the compounds where hydroxy and amide functions have been interchanged. Compared to 2'-acetylpaclitaxel (**67**) those more bulky compounds (**32**, **34**, **35**, **36**) retain an amide proton, which might act as a hydrogen bond donor. The significant difference in the binding affinity of 2'-deoxypaclitaxel (**90**) and 2'-deoxydocetaxel (**87**) (actual ratio: 2.3) might be due to an intramolecular hydrogen bond[10] that is necessary to stabilize the side chain of paclitaxel (**1**), but not of the more bulky *t*-BOC group of docetaxel (**39**).

The lack of steric or electrostatic interactions around C-7 and the regions around the 3'-phenyl and the 3'-*N*, where bulk is not tolerated, may explain why there are no compounds reported in the literature, that are much more active than **1** or **39**. Furthermore the very poor activity of the two photoaffinity labeling compounds (**10**, **11**), that possess an azidobenzoyl moiety at C-7, underscores that larger groups probably will cause a negative steric interaction.

Conclusion.

We generated a 3-D QSAR model which not only has the ability to explain the activity of already known compounds but has an excellent predictive power to forecast the biological activity of new compounds within the range of the data set.[13] Further improvement of the model should easily be possible by increasing the variety of structural properties (*e.g.* modifications at the 2-benzoyl moiety, the oxetane ring or other parts of the skeleton) in the data set and by using a force field which better accounts for hydrogen bonding and hydrophobic interactions.

Acknowledgments.

We thank Dr. G. I. Georg (Department of Medicinal Chemistry, University of Kansas) for the structural data and Dr. R. A. Himes (Department of Biochemistry, University of Kansas) for the biological data of all unpublished compounds. K.-H. A. Czaplinski was supported by a Kansas Health Foundation cancer scholar grant and the Research Development Fund at the University of Kansas.

Figure 1. Structure of the paclitaxel analogues used.

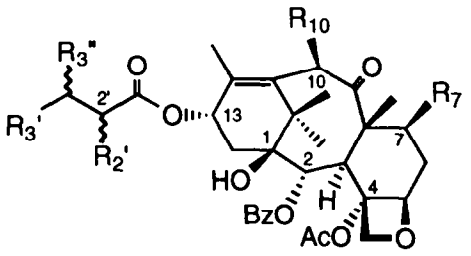

Table 1. Structures used for calculating the CoMFA model (training set of 50 compounds).

#	stereo-chemistry	R3'	R3"	R2'	R10	R7	ratio[d]	log (1/ratio)	ref.
1	2'*R*, 3'*S*	Ph	BzNH	OH	OAc	OH	1.0	0.0000	15
2	2'*R*, 3'*S*	Ph	BzNH	OH	OH	OH	1.3	-0.1139	15
4	2'*R*, 3'*S*	Ph	BzNH	OH	OAc	β-XylosylO	0.4	0.3979	16
5	2'*R*, 3'*S*	Ph	BzNH	OH	OAc	OBz	1.7	-0.2304	17
7	2'*R*, 3'*S*	Ph	BzNH	OH	OH	β-XylosylO	0.6	0.2218	16
8[c]	2'*R*, 3'*S*	Ph	BzNH	OH	OAc	Glutarate	1.0	0.0000	15
9[c]	2'*R*, 3'*S*	Ph	*t*-BOCNH	OH	OH	Phenylalaninate	1.0	0.0000	15
13[c]	2'*R*, 3'*S*	Ph	*t*-BOCNH	OH	Glycinate	Glycinate	1.2	-0.0792	15
14[a]	2'*R*, 3'*S*	Ph	BzNH	OH	OAc	OH	0.8	0.0969	18
18[b]	2'*R*, 3'*S*	Ph	BzNH	OH	OAc	OH	3.0	-0.4771	19
21	2'*R*, 3'*S*	4-ClPh	BzNH	OH	OAc	OH	1.9	-0.2788	20
22	2'*R*, 3'*S*	4-FPh	BzNH	OH	OAc	OH	1.1	-0.0414	5
23	2'*R*, 3'*S*	4-MePh	BzNH	OH	OAc	OH	2.4	-0.3802	21
24	2'*R*, 3'*S*	4-HOPh	BzNH	OH	OAc	OH	0.8	0.0969	22
25	2'*R*, 3'*S*	4-MeOPh	BzNH	OH	OAc	OH	0.5	0.3010	5
26	2'*R*, 3'*S*	2-Naphthyl	BzNH	OH	OAc	OH	7.1	-0.8513	5
31	2'*R*, 3'*S*	3-ClPh	BzNH	OH	OAc	OH	4.4	-0.6435	5
32	2'*R*, 3'*S*	Ph	OH	BzNH	OAc	OH	10	-1.0000	15
34	2'*R*, 3'*S*	Ph	OH	BzNH	OH	OH	10	-1.0000	15
35	2'*R*, 3'*S*	Ph	OH	*t*-BOCNH	OAc	OH	10	-1.0000	15
36	2'*R*, 3'*S*	Ph	OH	*t*-BOCNH	OH	OH	10	-1.0000	15
37	2'*R*, 3'*S*	Ph	3-ClBzNH	OH	OAc	OH	2.0	-0.3010	23
39	2'*R*, 3'*S*	Ph	*t*-BOCNH	OH	OH	OH	0.5	0.3010	15
44[c]	2'*R*, 3'*S*	Ph	GlutarylNH	OH	OH	OH	1.0	0.0000	15
47	2'*R*, 3'*S*	Ph	4-ClBzNH	OH	OAc	OH	2.4	-0.3802	20
50	2'*R*, 3'*S*	Ph	*n*-BuOCONH	OH	OAc	OH	0.8	0.0969	5
51	2'*R*, 3'*S*	Ph	4-MeBzNH	OH	OAc	OH	1.6	-0.2041	21
54	2'*R*, 3'*S*	Ph	4-CF_3BzNH	OH	OAc	OH	6.0	-0.7782	21
55	2'*R*, 3'*S*	Ph	4-MeOBzNH	OH	OAc	OH	0.6	0.2218	23
56	2'*R*, 3'*S*	Ph	PyruvoylNH	OH	OAc	OH	3.5	-0.5441	5
62	2'*R*, 3'*S*	Ph	*t*-ButylacetylNH	OH	OAc	OH	0.7	0.1549	24
67	2'*R*, 3'*S*	Ph	BzNH	OAc	OAc	OH	30	-1.4771	16
68	2'*R*, 3'*S*	Ph	*t*-BOCNH	OAc	OH	OH	10	-1.4771	14
69[c]	2'*R*, 3'*S*	Ph	NH_2	OH	OAc	OH	44	-1.6435	15
71	2'*S*, 3'*R*	Ph	BzNH	OH	OH	OH	4	-0.6021	15
72	2'*S*, 3'*R*	Ph	*t*-BOCNH	OH	OAc	OH	30	-1.4771	15
73	2'*S*, 3'*R*	Ph	*t*-BOCNH	OH	OH	OH	30	-1.4771	15
74	2'*S*, 3'*R*	Ph	OH	BzNH	OAc	OH	110	-2.0414	15
75	2'*S*, 3'*R*	Ph	OH	BzNH	OH	OH	170	-2.2304	15
76	2'*S*, 3'*R*	Ph	OH	*t*-BOCNH	OAc	OH	108	-2.0334	15
77	2'*S*, 3'*R*	Ph	OH	*t*-BOCNH	OH	OH	160	-2.2041	15
78	2'*R*, 3'*R*	Ph	BzNH	OH	OH	OH	1.3	-0.1139	15
79[c]	2'*R*, 3'*R*	Ph	NH_2	OH	OH	OH	30	-1.4771	15
80[c]	2'*S*, 3'*S*	Ph	NH_2	OH	OH	OH	30	-1.4771	15
81	2'*S*, 3'*S*	Ph	BzNH	OH	OH	OH	1.3	-0.1139	15
82	2'*R*, —	Ph	H	OH	OH	OH	4.5	-0.6532	15
88	2'*S*, —	Ph	H	OH	OH	OH	3.5	-0.5441	15
91	—, —	Ph	H	H	OH	OH	17	-1.2304	15
92	trans	Me	double	bond	OAc	OH	100	-2.0000	15
93	trans	Ph	double	bond	OH	OH	23	-1.3617	15

[a]9-dihydropaclitaxel. [b](1α)-15(16)-anhydro-11(15→1)-abeopaclitaxel. [c]charged species were used. [d]ID_{50}(compound)/ID_{50}(paclitaxel).[3]

Table 2. Statistics for the CoMFA approach for the compounds of **Table 1**.

model[a]	# of cv groups[b]	# of comp.[c]	r^2	standard error	F value	bootstrapping (n=100):	
	50	6	0.842	0.317	38.2	r^2	0.971 ± 0.009
b6	0	6	0.957	0.164	161.4	standard error	0.133 ± 0.070
	50	4	0.853	0.298	65.5	r^2	0.967 ± 0.009
wb4	0	4	0.958	0.159	259.5	standard error	0.139 ± 0.069
	50	4	0.825	0.326	52.9	r^2	0.957 ± 0.012
e4	0	4	0.939	0.193	172.8	standard error	0.159 ± 0.079
	50	4	0.814	0.336	49.3	r^2	0.950 ± 0.015
s4	0	4	0.936	0.196	165.8	standard error	0.171 ± 0.086

[a]model[9] calculated using **b6**: both fields (default), **wb4**: both fields (with electrostatics at sterically bad points), **e4**: electrostatic field (default), **s4**: steric field (default). [b]number of crossvalidation groups. [c]number of components.

Table 3. Predicting the biological activity of compounds using the CoMFA model.

#	stereo-chemistry	R3'	R3"	R2'	R10	R7	actual ratio[a]	predicted ratios[a] b6	wb4	e4	s4	ref.
3	2'*R*, 3'*S*	Ph	BzNH	OH	OAc	OAc	2.0	1.2	1.0	0.9	1.2	16
6	2'*R*, 3'*S*	Ph	BzNH	OH	OAc	4-($CF_3(N_2C)$)BzO	3.4	1.8	1.7	1.3	2.5	17
10[g]	2'*R*, 3'*S*	Ph	BzNH	OH	OAc	4-N_3BzO	21.4	1.7	1.6	1.2	2.3	25
11[g]	2'*R*, 3'*S*	Ph	BzNH	OH	OAc	4-N_3F_4BzO	> 22.4	1.6	1.3	0.8	2.3	26
12	2'*R*, 3'*S*	Ph	TigloylNH	OH	OAc	β-XylosylO	0.5	0.7	0.7	0.9	0.9	16
15[h]	2'*R*, 3'*S*	Ph	*t*-BOCNH	OH	Glutarate	Glutarate	2.0	0.4	0.5	0.3	0.7	15
16	2'*R*, 3'*S*	Ph	*t*-BOCNH	OH	TrocO	TrocO	> 39	0.5	0.6	0.8	0.9	5
17	2'*R*, 3'*S*	Ph	BzNH	OH	H	OH	143[c]	2.1	2.4	1.6	2.4	27
19[b]	2'*R*, 3'*S*	Ph	BzNH	OH	—	OH	106[c]	1.3	2.0	2.0	1.4	27
20	2'*R*, 3'*S*	2-Furyl	BzNH	OH	OAc	OH	0.9	3.9	4.0	3.7	5.4	28
27	2'*R*, 3'*S*	3-Furyl	BzNH	OH	OAc	OH	0.9	2.2	2.7	3.2	2.2	28
28	2'*R*, 3'*S*	2-Pyridyl	BzNH	OH	OAc	OH	0.7	1.7	2.0	1.6	2.3	28
29	2'*R*, 3'*S*	3-Pyridyl	BzNH	OH	OAc	OH	0.5	1.6	1.7	1.4	1.8	28
30	2'*R*, 3'*S*	4-Pyridyl	BzNH	OH	OAc	OH	0.4	1.6	1.6	1.5	1.6	28
33	2'*R*, 3'*S*	3,4-Cl_2Ph	BzNH	OH	OAc	OH	7.1	3.2	3.1	2.9	2.6	5
38	2'*R*, 3'*S*	2-Furyl	*t*-BOCNH	OH	OAc	OH	1.7	2.0	1.7	2.2	2.6	5
40	2'*R*, 3'*S*	Ph	*t*-BOCNH	OH	OAc	OH	0.5	0.5	0.6	1.0	0.7	15
41	2'*R*, 3'*S*	Ph	TigloylNH	OH	OAc	OH	1.5	1.3	1.7	2.1	1.7	29
42	2'*R*, 3'*S*	Ph	TigloylNH	OH	OH	OH	5.0	1.2	1.5	1.4	1.4	29
43	2'*R*, 3'*S*	Ph	4-NO_2BzNH	OH	OAc	OH	2.0	2.3	2.5	2.6	1.8	23
45	2'*R*, 3'*S*	Ph	4-FBzNH	OH	OAc	OH	1.2	1.4	1.2	1.3	1.2	23
46	2'*R*, 3'*S*	Ph	3,4-Cl_2BzNH	OH	OAc	OH	2.1	1.7	1.4	1.3	1.5	23
48	2'*R*, 3'*S*	Ph	2-MeBzNH	OH	OAc	OH	1.9	1.4	1.4	1.8	1.1	23
49	2'*R*, 3'*S*	Ph	3-N(Me)$_2$BzNH	OH	OAc	OH	1.4	1.4	1.2	1.2	1.3	23
52	2'*R*, 3'*S*	Ph	MeC(NNH-*t*-BOC)CONH	OH	OAc	OH	14.1	7.0	7.0	4.1	13.7	5
53	2'*R*, 3'*S*	Ph	MeC(NOH)CONH	OH	OAc	OH	3.5	2.8	2.1	2.1	3.3	5
57	2'*R*, 3'*S*	Ph	2-FuroylNH	OH	OAc	OH	0.8	1.5	1.5	1.4	1.6	5
58	2'*R*, 3'*S*	Ph	3-FuroylNH	OH	OAc	OH	0.4	2.3	2.0	1.7	2.8	5
59	2'*R*, 3'*S*	Ph	Me_3CCONH	OH	OAc	OH	2.6	1.4	1.3	1.4	2.0	24
60	2'*R*, 3'*S*	Ph	IsovalerylNH	OH	OAc	OH	1.2	0.8	1.1	2.0	1.1	24
61	2'*R*, 3'*S*	Ph	$C_5H_{11}CONH$	OH	OAc	OH	0.4	0.7	0.9	1.5	0.8	5
63	2'*R*, 3'*S*	Ph	BnOCONH	OH	OAc	OH	3.3	2.7	2.9	2.4	3.8	5
64[g]	2'*R*, 3'*S*	Ph	4-N_3BzNH	OH	OAc	OH	2.0	1.4	1.1	1.0	1.3	26
65[g]	2'*R*, 3'*S*	Ph	4-N_3F_4BzNH	OH	OAc	OH	4.6	1.4	1.0	1.1	1.3	26
66	2'*S*, 3'*R*	Ph	BzNH	OH	OAc	OH	4.5	2.4	3.5	5.0	2.8	15
70	2'*R*, —	H	BzNH	OH	OAc	OH	5.6[c]	14.3	9.7	5.6	10.9	10
83	2'*R*, —	Ph	H	OH	OAc	OH	13.2[c]	3.7	3.1	4.2	6.3	10
84	2'*R*, —	H	H	OH	OAc	OH	5.6[c]	29.4	23.9	17.5	64.7	10
85	2'*S*, —	H	H	OH	OAc	OH	6.4[c]	46.6	34.2	22.5	68.6	10
86	2'*S*, —	Ph	H	OH	OAc	OH	15.7[c]	5.7	6.6	11.4	7.2	10
87	—, 3'*S*	Ph	*t*-BOCNH	H	OH	OH	2.3	0.7	0.9	1.5	0.6	14
89	—, 3'*R*	Ph	*t*-BOCNH	H	OAc	OH	4.1	9.7	14.4	7.3	16.3	14
90	—, 3'*S*	Ph	BzNH	H	OAc	OH	21.2	1.6	1.7	2.1	1.3	11,12
94	trans	Ph	double bond		TrocO	TrocO	1000	25.5	21.5	22.2	35.4	15
95[d]	—, —	—	—		OAc	OH	52	96.4	76.8	45.0	162.2	16
96[e]	3'*R*, 4'*S*	Ph	BzNH	OH	OH	OH	> 27	20.2	32.4	24.1	33.1	30
97[f]	3'*R*, 4'*S*	Ph	*t*-BOCNH	OH	OH	OH	> 27	10.5	24.4	21.6	15.2	30

[a]ID_{50}(compound)/ID_{50}(paclitaxel). [b]10-deacetoxy-10,11-12,18-tetradehydropaclitaxel. [c]initial slope of tubulin[3] polymerization. [d]baccatin III. [e]C-13 side chain: 4-benzoylamino-3-hydroxy-4-phenylbutyryl. [f]C-13 side chain: 4-*t*-butoxycarbonylamino-3-hydroxy-4-phenylbutyryl. [g]see ref. 31. [h]charged species was used

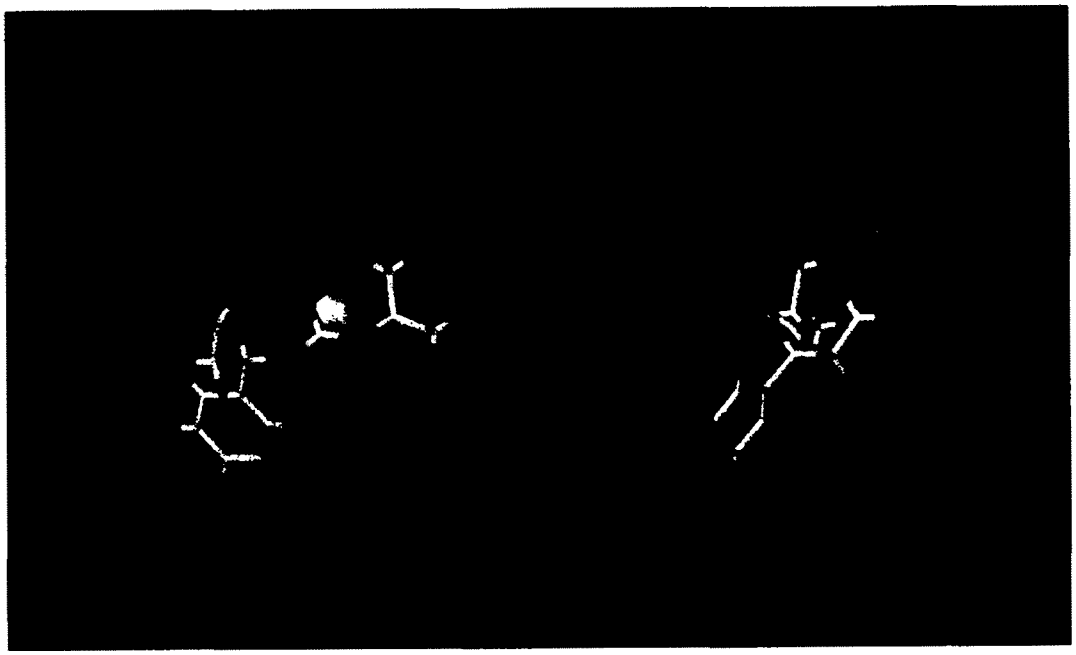

Figure 2 (left): Steric contour plot; (right): Steric contour plot, orthographic view. The positive contours are shown in green and the negative contours are shown in magenta. The contours were drawn at a 0.013 level.

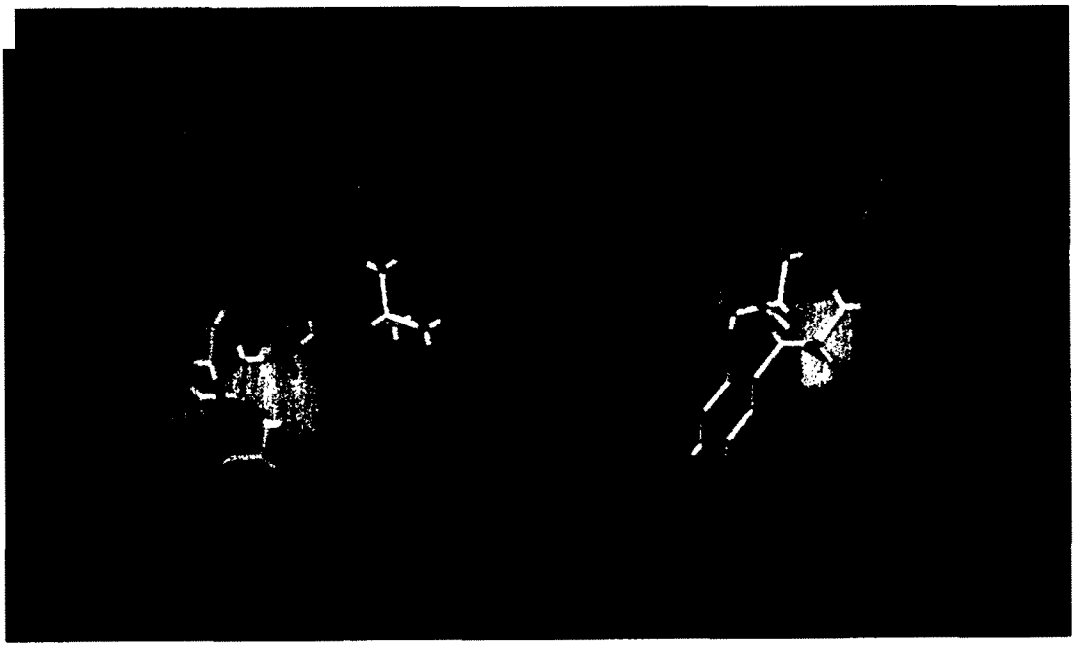

Figure 3 (left): Electrostatic contour plot; (right): Electrostatic contour plot, orthographic view. The positive contours are shown in cyan and the negative contours are shown in orange. The contours were drawn at a 0.013 level.

References and Notes.

1. Presented at the 207th National Meeting of the American Chemical Society (San Diego, CA, March 13, 1994, Abstract MEDI 105).
2. Cramer, R. D.; Patterson, D. E. and Bunce, J. D. *J. Am. Chem. Soc.* **1988**, *110*, 5959.
3. (a) The ratios [ID_{50}(compound)/ID_{50}(taxol)] from the microtubule assembly assay and the microtubule disassembly assay were used to make the activity data comparable; (b) for a review of the in vitro microtubule assays (assembly and disassembly), see reference 21.
4. Georg, G. I.; Boge, T. C.; Cheruvallath, Z. S.; Clowers, J. S.; Harriman, G. C. B.; Hepperle, M. and Park, H. *Taxol: Science and Applications*; Suffness, M., Ed.; CRC Press, Inc.: Boca Raton, 1993 (in press).
5. Georg, G. I.; Himes, R. A. and collaborators (unpublished results) **1993/1994**. Activity data are from the microtubule assembly assay.
6. SYBYL 6.0, Tripos Associates, St. Louis, MO.
7. (a) CSD, Cambridge Crystallographic Data Centre, Lensfield Road, Cambridge CB2 1EW, U.K., REFC= VEJCUI; (b) Guéritte-Voegelein, F.; Guénard, D.; Mangatal, L.; Potier, P.; Guilhem, J.; Cesario, M. and Pascard, C. *Acta Crystallogr.* **1990**, *C46*, 781.
8. MOPAC 5.0 (QCPE program # 455); Frank J. Seiler Res. Lab., U.S. Air Force Academy, Colorado Springs, CO 80840.
9. (a) model **b6**: both fields, no electrostatics at sterically bad points, optimum number of components is 6 as given by CoMFA; (b) model **wb4**: both fields, with electrostatics at sterically bad points, optimum number of components is 4 instead of 10 (less complex model with almost the same statistical quality); (c) model **e4**: electrostatic field only (other setup: default), optimum number of components is 4 instead of 7 (less complex model with almost the same statistical quality); (d) model **s4**: steric field only (other setup: default), optimum number of components is 4 instead of 10 (less complex model with almost the same statistical quality).
10. Swindell, C. S.; Krauss, N. E.; Horwitz, S. B. and Ringel, I. *J. Med. Chem.* **1991**, *34*, 1176.
11. Kant, J.; Huang, S.; Wong, H.; Fairchild, C.; Vyas, D. and Farina, V. *Bioorg. Med. Chem. Lett.* **1993**, *3*, 2471.
12. Personal communication of Dr. J. Kant, Bristol-Myers Squibb Pharmaceutical Research Institute.
13. Because there is only a small range in the actual activity data of the compounds in **Table 3** (with structural properties within the range of the training set) used for predicting the activity, these CoMFA models can be refined as new data become available.
14. Dubois, J.; Guénard, D.; Guéritte-Voegelein, F.; Guedira, N.; Potier, P.; Gillet, B.; Beloeil, J.-C. *Tetrahedron* **1993**, *49*, 6533.
15. Guéritte-Voegelein, F.; Guénard, D.; Lavelle, F.; Le Goff, M.-T.; Mangatal, L. and Potier, P. *J. Med. Chem.* **1991**, *34*, 992.
16. Lataste, H.; Sénilh, V.; Wright, M.; Guénard, D. and Potier, P. *Proc. Natl. Acad. Sci. U.S.A.* **1984**, *81*, 4090.
17. Kingston, D. G. I.; Samaranayake, G. and Ivey, C. A. *J. Nat. Prod.* **1990**, *53*, 1.
18. Klein, L. *Tetrahedron Lett.* **1993**, *34*, 2047.
19. Samaranayake, G.; Magri,.N. F.; Jitrangsri, C. and Kingston, D. G. I. *J. Org. Chem.* **1991**, *56*, 5114.
20. Georg, G. I.; Cheruvallath, Z. S.; Himes, R. A. and Mejillano, M. R. *Bioorg. Med. Chem. Lett.* **1992**, *2*, 295.
21. Georg, G. I.; Cheruvallath, Z. S.; Himes, R. A. and Mejillano, M. R. *Bioorg. Med. Chem. Lett.* **1992**, *2*, 1751.
22. Monsarrat, B.; Mariel, E.; Cros, S.; Garés, M.; Guénard, D.; Guéritte-Voegelein, F. and Wright, M. *Drug Metab. Dispos.* **1990**, *18*, 895.
23. Georg, G. I.; Boge, T. C.; Cheruvallath, Z. S.; Harriman, G. C. B.; Hepperle, M.; Park, H. and Himes, R. H. *Bioorg. Med. Chem. Lett.* **1994**, *4*, 1825.
24. Georg, G. I.; Boge, T. C.; Cheruvallath, Z. S.; Harriman, G. C. B.; Hepperle, M.; Park, H. and Himes, R. H. *Bioorg. Med. Chem. Lett.* **1994**, *4*, 335.
25. Georg, G. I.; Harriman, G. C. B.; Himes, R. A. and Mejillano, M. R. *Bioorg. Med. Chem. Lett.* **1992**, *2*, 735.
26. Georg, G. I.; Harriman, G. C. B.; Park, H. and Himes, R. A. *Bioorg. Med. Chem. Lett.* **1994**, *4*, 487.
27. Chen, S.-H.; Fairchild, C.; Mamber, S. W. and Farina, V. *J. Org. Chem.* **1993**, *58*, 2927.
28. Georg, G. I.; Harriman, G. C. B.; Hepperle, M. and Himes, R. H. *Bioorg. Med. Chem. Lett.* **1994**, *4*, 1381; (**27** assayed as a 3:1 diastereomeric mixture; **29** assayed as a 2:1 diastereomeric mixture).
29. Chauviere, G.; Guénard, D.; Picot, F.; Sénilh, V. and Potier, P. *C. R. Seances Acad. Sci.*, **1981**, Ser. 2, *293*, 501.
30. Jayasinghe, L. R.; Datta, A.; Ali, S. M.; Zygmunt, J.; Georg, G. I. and Vander Velde, D. *J. Med. Chem.* **1994**, (accepted).
31. The geometry of the azido group was taken from Magnoli, A.; Mariani, C. and Simonetta, M. *Acta Crystallogr.* **1965**, *19*, 367.

(*Received in USA* 7 *July* 1994; *accepted* 18 *August* 1994)